J Mol Med (2013) 91:951–963
DOI 10.1007/s00109-013-1015-3

JMolMed

ORIGINAL ARTICLE

Proximal tubule specific knockout of the Na^+/H^+ exchanger NHE3: effects on bicarbonate absorption and ammonium excretion

Hong C. Li · Zhaopeng Du · Sharon Barone · Isabelle Rubera · Alicia A. McDonough · Michel Tauc · Kamyar Zahedi · Tong Wang · Manoocher Soleimani

Received: 19 October 2012 / Revised: 16 January 2013 / Accepted: 25 February 2013 / Published online: 19 March 2013

Abstract The existing NHE3 knockout mouse has significant intestinal electrolyte absorption defects, making this model unsuitable for the examination of the role of proximal tubule NHE3 in pathophysiologic states in vivo. To overcome this problem, we generated proximal convoluted tubule-specific KO mice (NHE3-PT KO) by generating and crossing NHE3 floxed mice with the sodium-glucose transporter 2 Cre transgenic mice. The NHE3-PT KO mice have >80 % ablation of NHE3 as determined by immunofluorescence microscopy, western blot, and northern analyses, and show mild metabolic acidosis (serum bicarbonate of 21.2 mEq/l in KO vs. 23.7 mEq/l in WT, $p<0.05$). In vitro microperfusion studies in the isolated proximal convoluted tubules demonstrated a ~36 % reduction in bicarbonate reabsorption (J_{HCO3}=53.52±4.61 pmol/min/mm in KO vs. 83.09±9.73 in WT) and a ~27 % reduction in volume reabsorption (J_v=0.67±0.07 nl/min/mm in KO vs. 0.92±0.06 nl/min/mm in WT) in mutant mice. The NHE3-PT KO mice tolerated NH_4Cl acid load well (added to the drinking water) and showed NH_4 excretion rates comparable to WT mice at 2 and 5 days after NH_4Cl loading without disproportionate metabolic acidosis after 5 days of acid load. Our results suggest that the Na^+/H^+ exchanger NHE3 plays an important role in fluid and bicarbonate reabsorption in the proximal convoluted tubule but does not play an important role in NH_4 excretion.

Keywords Metabolic acidosis · Kidney tubules · Bicarbonate absorption · Salt absorption · Acid loading

H. C. Li · S. Barone · K. Zahedi · M. Soleimani (✉)
Center on Genetics of Transport and the Department of Medicine, University of Cincinnati, Cincinnati, OH, USA
e-mail: manoocher.soleimani@uc.edu

Z. Du · T. Wang
Department of Cellular and Molecular Physiology, Yale University, New Haven, CT, USA

I. Rubera · M. Tauc
Université de Nice Sophia Antipolis, Nice, France

A. A. McDonough
Department of Cell and Neurobiology, University of Southern California, Los Angeles, CA, USA

H. C. Li · S. Barone · A. A. McDonough · M. Soleimani
Research Services, Veterans Affairs Medical Center, Cincinnati, OH, USA

Introduction

The sodium hydrogen exchanger NHE3, encoded by solute-linked carrier family 9, member 3 gene, is abundantly expressed in the intestine and kidney tubules [1–3]. NHE3 is expressed on the villi in the apical membrane of epithelial cells in both small and large intestines [3–5]. NHE3 expression in the kidney is limited to the proximal tubule and thick ascending limb of Henle [1, 6–9], two segments that play important role in salt and bicarbonate reabsorption [9–13].

In the kidney proximal tubule, NHE3 is located on the apical membrane of cells along the length of tubule, extending from S1 and S2 segments (convoluted tubule) to the S3 segment (straight tubule). NHE3 is also expressed on the apical membrane of cells in the thick ascending limb of Henle [7, 14]. Its main role in the S1 and S2 segments of the proximal tubules is the reabsorption of fluid and bicarbonate. As a result, NHE3 is thought to be important in vascular volume homeostasis and acid base balance [15, 16]. In the

S3 segment, NHE3 is predominantly involved with volume absorption with no significant impact on bicarbonate absorption [17–21]. In the thick ascending limb, NHE3 is thought to play an important role in salt absorption and overall fluid and electrolyte maintenance [6, 22]. NHE3 is also the main sodium-absorbing transporter along the length of the small intestine and colon [23].

The conventional (global) NHE3 KO mice display significant fluid absorption defect in the gastrointestinal tract, resulting in vascular volume depletion, and as a consequence reduced kidney perfusion and function [24, 25]. In addition, the impaired bicarbonate absorption in the small intestine may contribute to the metabolic acidosis that is observed in the mutant mice [22, 24, 26, 27]. These abnormalities, predominantly due to fluid and electrolyte loss in the intestine, can modulate many systemic signaling and transport pathways in other tissues, including the kidney tubules. As such, the tubular transport abnormalities in the NHE3 KO mice might in part reflect the secondary phenotype subsequent to the aforementioned derangements. Further, the profound fluid loss in the intestine in conjunction with reduced kidney perfusion (reduced glomerular filtration rate (GFR) [24]) makes it impossible to study the role of kidney proximal tubule NHE3 in many pathophysiologic states in vivo, specifically those conditions requiring challenge test with acid, bicarbonate or salt, as the intestinal absorption and kidney filtration and secretion of these chemicals are impaired in NHE3 KO mice.

To circumvent the defect in fluid absorption in the intestine in NHE3 KO mice and investigate the role of NHE3 in the renal proximal tubules in pathophysiologic states in vivo, we generated proximal convoluted tubule specific NHE3 KO mice. This animal model provides us with a unique tool to study the role of proximal tubule NHE3 in fluid and bicarbonate reabsorption in pathophysiologic states.

Experimental procedures

Generation of conditional NHE3 knockout mice

An NHE3 conditional targeting vector containing the NHE3 genomic region was constructed, in which the negative selective marker thymidine kinase gene, and the positive selective marker neomycin resistance (neo cassette) gene flanked by two Frt sites and two floxed sites were introduced in relevant positions. The vector was designed to flox exons 4 and 5, flanked by 2.3 and 3.2 kb short and long homology arms, respectively. The linearized targeting vector was electroporated into 129/SvOla ES cells [28]. After dual selections by G418 and ganciclovir and screening by genomic PCR, ES cells containing NHE3 conditional targeted allele were identified. The identity of ES cells was further confirmed by Southern blot analysis.

Two correctly targeted ES cell clones were used for blastocyst injection to generate chimeric mice, which were then crossed with WT C57BL/6 mice to obtain mice capable of germ line transmission of NHE3 conditional knockout gene (ES cell electroporation and blastocyst injection were performed by the Gene Targeting Mouse Service Core at the University of Cincinnati). The animals were bred with Flp recombinase transgenic mice to obtain conditional NHE3 KO mice with floxed allele lacking the neo cassette. These mice were crossed with wild-type C57BL/6 mice to remove Flp recombinase transgene in order to generate mice heterozygote for NHE3 conditional knockout gene ($NHE3^{+/fl}neo^{-}flp^{-}$), which are designated as $NHE3^{fl/fl}$ or $NHE3^{+/fl}$ mice. These animals were mated with sodium-glucose transporter 2 (Sglt2) promoter-driven Cre recombinase transgenic mice in order to disrupt NHE3 gene expression in the S1 and S2 regions of the proximal tubule [29].

PCR analysis Genomic DNA isolated from ES cells containing NHE3 conditional targeted allele was screened by PCR analysis, yielding a 2.9 kb DNA fragment. $LoxP^{+}$, Neo^{+}, Flp^{+}, and Cre^{+} alleles were identified by PCR analysis of the genomic DNA. All PCR reactions were performed using the AccuPrime Taq DNA Polymerase System PCR kit with buffer II (Invitrogen, Carlsbad, CA, USA). Primers PS.1659 and PS.1660 were used to identify NHE3 $LoxP^{+}$ allele ($LoxP^{+}$, 250 bp; $LoxP^{-}$ or wild type, 200 bp). Neo-Pr1 sense and E4E5 antisense primers were used to determine the presence of Neo cassette (Neo^{+}, 2.7 kb; Neo^{-}, 1.3 kb DNA fragments). Flp sense and antisense primers were used to identify Flp sequence, resulting in 0.7 kb (Flp^{+}) and 0.3 kb (wild type) DNA fragments. The primers used in these studies are included in Table 1. Cre 391 sense and antisense were used to determine the presence of Cre recombinase transgene (Cre^{+}, 391 bp; Cre^{-}, 245 bp) [29]. The Neo cassette-disrupted NHE3 gene allele from $NHE3^{-/fl}$ and $NHE3^{+/-}$ conventional knockout mice were genotyped by PCR amplification of genomic DNA with primers F, R, and N [24]. Two distinct products, a 200 bp band indicating the presence of wild type and a 160-bp fragment indicating the presence of Neo cassette-disrupted NHE3 gene, were used to identify the genetic make-up of the animals [24]. A PCR fragment (257 bp) generated from mouse kidney cDNA with NHE3 257 sense and antisense primers was used as the probe for northern blot analyses. Cycling parameters for all PCR screening experiments were as follows: segment 1–95 °C, 30 s (one cycle) and segment 2–95 °C, 30 s, 60 °C, 1 min, 68 °C, 3 min (40 cycles).

Microperfusion of proximal tubules in vitro The experiments were conducted under animal protocol 2007–10473 (TW) approved by the Institutional Animal Care and Use Committee. Proximal convoluted tubules (S_2 segments)

Table 1 Primer sequences for generating NHE3 proximal tubule specific conditional knock-out mice

NHE_3 2.9 kb sense	5′AGGGTGGGTACTATTGGTCACATTGG3′
NHE_3 2.9 kb antisense	5′GCTACCCGTGATATTGCTGAAGAGC3′
PS. 1659	5′AGCCAAGGATAATTCTGAAGAC3′
PS. 1660	5′TGCCTACTGTTCCTTGGTGAAG3′
Neo-Pr1 sense	5′GACTACATGGTAGAGGGCATTGGCTTG3′
E4E5 reverse	5′TCTAGAACTAGTGGATCCCC3′
Flp sense	5′CACTGATATTGTAAGTAGTTTGC3′
Flp antisense	5′CTAGTGCGAAGT AGTGATCAGG3′
Cre 391 sense	5′CCTGGAAAATGCTTCTGTCCG3′
Cre 391 antisense	5′CAGGGTGTTATAAGCAATCCC3′
Myogenic sense	5′TTACGTCCATCGTGGACAGC3′
Myogenic antisense	5′TGGGCTGGGTGTTAGTCTTA3′
NHE_3 primer F	5′CTTTTGCGGCATCTGCTGTCA3′
NHE_3 primer R	5′CAGAAATGAAGACCAGTGTCA3′
NHE_3 primer N	5′ GCATGCTCCAGACTGCCTTG 3′
NHE_3 257 sense	5′GTCTTGTACAATGTTTTTGAGT3′
NHE_3 257 antisense	5′GCCAGGATGGATGACAAAGACAGCAT3′

were perfused in vitro using conventional methods [30]. Briefly, age-matched animals from either WT or proximal tubule (NHE3 PT) KO mice were anesthetized by an intraperitoneal injection of 50 mg/kg body wt of pentobarbital sodium. Then kidneys were removed and cut into coronal slices and individual tubules were dissected in cooled (4 °C) Hanks' solution containing (in millimolar) 137 NaCl, 5 KCl, 0.8 $MgSO_4$, 0.33 Na_2HPO_4, 1 $MgCl_2$, 10 Tris, 0.25 $CaCl_2$, 2 glutamine, and 2 L-lactic acid. Proximal tubules (S_2) were perfused with an ultrafiltrate-like solution. The perfusion rates were adjusted by changing the height of the reservoir connected to the perfusion pipette and measured by a calibrated collection pipette. The solution for luminal perfusion contained (in millimolar) 125 NaCl, 22 $NaHCO_3$, 1 $CaCl_2$, 1.2 $MgSO_4$, 2 glutamine, 2 lactic acid, 5 KCl, and 1.2 phosphoric acid. The bath medium consisted of (millimolar) 101 NaCl, 22 $NaHCO_3$, 1 $CaCl_2$, 1.2 $MgSO_4$, 2 glutamine, 2 lactic acid, 10.5 glucose, 5 KCl, 1.2 phosphoric acid, and 32.5 HEPES as well as 5 g/dl albumin. All solutions were bubbled with 95 % O_2–5 % CO_2 and had a pH of 7.4. The osmolalities of the bath and luminal solution were adjusted to 300 mOsmol/kg H_2O by the addition of either H_2O or NaCl. Extensively dialyzed [methoxy-^{3}H]-inulin was added to the perfusate at a concentration of 30 μCi/ml as a volume marker [30]. Tubular fluid collection began after an equilibration time of 30–60 min and a total of four timed collections were made for measuring fluid and bicarbonate absorption. The volume of the perfusate and collected samples was measured and [^{3}H]-inulin concentrations in those samples were determined using a liquid scintillation counter. The rate of net fluid reabsorption (J_v) was calculated according to the [^{3}H]-inulin concentration changes between the original and collected fluid. The HCO_3^- concentration in the perfusate and collected tubular fluid was measured by microfluorometry (Nanoflow; World Precision Instruments, Sarasota, FL, USA). The rate of HCO_3^- absorption (J_{HCO3}) was calculated according to the HCO_3^- concentration changes between the original and collected fluid. The J_v and J_{HCO3} are expressed as per minute per millimeter of proximal tubule [30].

Immunofluorescent labeling Mice were euthanized with an overdose of pentobarbital sodium and perfused through the left ventricle with 0.9 % saline followed by cold 4 % paraformaldehyde in 0.1 M sodium phosphate buffer (pH7.4). Kidneys were removed, cut in tissue blocks, fixed in 4 % paraformaldehyde solution overnight at 4 °C, and then transferred to 30 % sucrose in 0.1 M sodium phosphate buffer (pH7.4) and stored at 4 °C. Kidneys were then embedded in O.C.T. compound (Saakura Finetek USA Inc., Torrance, CA, USA), frozen in liquid nitrogen, and 6-μm sections were cut using a cryostat. Frozen sections were stored at −80 °C until used. Single-immunofluorescence labeling was performed as described [31, 32] using either Alexa Fluor 488 (green) or Alexa Fluor 594 (red) (Invitrogen, Carlsbad, CA, USA) as secondary antibodies. NHE3 antibody was a purified high-specificity rabbit polyclonal antibody generated against a synthetic NHE3 peptide [33, 34].

Western blot The mouse kidney cortex tissues were cut and inserted in 2 ml round-bottom centrifuge tubes containing 2 % Triton X-100 lysis buffer. The samples were homogenized and centrifuged at 14,000×*g*. The resultant supernatant was saved and mixed with 2× Laemmli-loading buffer. The proteins were size fractionated by SDS PAGE and transferred to nitrocellulose membrane. Western blot analyses were performed according to established methods [35] using rabbit NHE3-specific polyclonal antibody at 1:500 dilution [34]. Donkey anti-rabbit IgG-horseradish peroxidase (HRP) was used as the secondary antibody at 1:1,000 dilution (Pierce, Rockford, IL, USA). For normalization of protein loading in western blot analysis, goat β-actin polyclonal antibody was used as primary antibody at 1:1,000 dilution (Santa Cruz Biotechnology, Santa Cruz, CA, USA) and mouse anti-goat IgG-HRP was used as the secondary antibody at 1:1,000 dilution (Pierce). The antigen–antibody complex was detected by chemiluminescence approach using Super Signal West Pico Chemiluminescent Substrate Kit (Pierce). The experiments were done in duplicate.

RNA isolation and northern blot hybridization Total cellular RNA was extracted from mouse kidney cortex and intestinal segments according to established methods, quantitated spectrophotometrically, and stored at −80 °C. Total RNA from each sample (20 μg/lane) was size fractionated on a

1.2 % agarose-formaldehyde gel, transferred to Magna NT nylon membranes, cross-linked by UV light, and baked. PCR-generated cDNA fragments specific for NHE3, glutamine dehydrogenase (GDH) or glutaminase were labeled with ^{32}P and used for northern blot analyses. Hybridization was performed according to established methods [21, 32]. The membranes were washed, blotted dry, and exposed to a PhosphorImager screen (Molecular Dynamics, Sunnyvale, CA, USA). The signal strength of hybridization bands was quantitated by densitometry using ImageQuaNT software (Molecular Dynamics, Sunnyvale, CA, USA).

Acid loading Animals were placed in metabolic cages and after acclimatization subjected to acid load by the addition of 280 mM NH_4Cl to their drinking water for 5 days. Urine was collected daily.

Systemic acid base analysis The blood pH and concentration of HCO_3^- and pCO_2 were measured using arterial blood and i-STAT^R-1 analyzer and i-STAT EG7+ cartridge (Abbott Laboratories, Abbot Park, IL, USA).

Blood and urine electrolyte analysis Mice were housed in metabolic cages and had free access to rodent chow and water. Food intake, water intake, and urine volume were measured daily. Urine was collected under mineral oil in order to avoid evaporation. Ammonium (NH_4^+) excretion was measured utilizing the phenol/sodium hypochlorite method described by Berthelot and previously used in our laboratory [21]. Serum and urine chloride concentration were measured with a digital chloridometer (HBI Haake Buchler Instruments). Concentrations of Na^+, K^+, Ca^{2+}, and HCO_3^- were measured in blood with an i-STAT^R-1 analyzer and i-STAT *EG7+* cartridges (Abbott Laboratories).

Blood pressure monitoring Systolic blood pressure in conscious mice was determined using a computerized tail-cuff sphygmomanometer (Visitech BP2000; Visitech Systems, Apex, NC, USA). Measurements for each mouse represent mean value of three consecutive recordings performed on three consecutive days. All experimental animals were acclimated to the procedure and the recording chamber for 3 days.

Statistics Data are presented as means±SE. ANOVA or Student's *t* test was used to compare experimental groups.

Results

Targeted inactivation of the mouse NHE3: generation of mice with germ line transmission of NHE3 conditional construct Figure 1a (left and right panels) depicts the targeting construct which is comprised of a phosphoglycerine kinase promoter driven Neo cassette flanked by FRT sites inserted between exon 3 and exon 4. Exons 4 and 5 are flanked by the two LoxP sites. The linearized targeting vector was electroporated into 129/SvOla ES cells [28]. Six ES cells that were correctly targeted by the vector were identified by PCR and Southern blot analysis. Figure 1b (left panel) demonstrates a PCR reaction on genomic DNA from electroporated ES cells and demonstrate the presence of three recombinant clones (clones 38, 48 and 123). Southern blot analysis of NsiI-digested ES cell genomic DNA confirmed the recombinant DNA in 6 ES clones (including clones 38, 48 and 123; Fig. 1b, right panel). The D38 ES clone was expanded and injected into C57BL/6 blastocysts. Two chimeric males were obtained and crossed with C57BL/6 females, generating several heterozygous NHE3^{floxneo} mice (Fig. 1c). The neo-cassette in NHE3$^{flox/neo}$ mice was removed by cross-mating with Flp positive mice (Fig. 1d).

Fig. 1 Targeted inactivation of the mouse NHE3 gene. **a** Schematic ▶ diagram of the mouse NHE3 genomic DNA and targeting vector (*left and right panels*). The mouse NHE3 exons 3–10 (designated E3, E4… E10) are shown in *rectangular boxes* in genomic DNA and important restriction enzyme sites used in DNA manipulation procedures are also indicated. The thymidine kinase (tk) cassette (designated as tk) was introduced upstream of exon 3 for negative selection of integrated clones. The neo cassette (designated as neo) flanked by two Frt sites (*left-pointing triangles*) was introduced between E3 and E4 in the targeting vector DNA. The two floxed sites were inserted upstream of E4 and downstream of E5, respectively, in the targeting vector (*right-pointing triangles*). As shown, the targeted allele is converted into floxed allele with a deletion of neo cassette and one Frt site upon Flp recombinase activation and the floxed allele is converted into conditional knockout allele by the removal of NHE3 exons 4 and 5 after Cre-mediated recombination, resulting in a nonfunctional NHE3 gene product with out of frame. **b** Identification of recombinant ES cells expressing conditional NHE3 KO construct. *Left panel* PCR reaction on genomic DNA from electroporated ES cells. Three recombinant clones (clones 38, 48, and 123) were identified by PCR reaction using specific primers (see "Experimental procedures"). *Right panel* Southern blot analysis of NHE3-targeted ES cells. The restriction enzymes Ssp I and Kpn I digested genomic DNA were hybridized with probe A upstream of exon 3 (Fig. 1a, *left panel*), which generated 7.3 kb wild-type and 8.9 kb mutant DNA bands, respectively. The restriction enzyme Nsi-digested genomic DNA was hybridized using probe B, downstream of exon 10 (Fig. 1a, *left panel*), which generated 6.5 kb wild-type and 4.5 kb mutant DNA bands, respectively. Southern blot analysis of NsiI-digested ES cell genomic DNA by probe B confirmed the recombinant DNA in 6 ES clones (including clones 38, 48, and 123). **a** Germline transmission of mice carrying the NHE3 conditional construct. After blastocyst injection and identification of chimeric mice with LoxP and Neo positive sites, NHE3 conditional knockout germ line mice were identified. Four mice (designated with *asterisk*) showed germ line transmission. **b** Generation of NHE3$^{+/fl-/neo-}$ mice (removal of neocassette). Mice capable of germ line transmission of NHE3 conditional construct were mated with C57BL/6 Flp-positive mice to remove the Neo cassette (as depicted in the schematic diagram in Fig. 1a). Genotyping was performed by PCR analysis of mouse tail genomic DNA using Neo-Pr1 forward and E4E5 reversal primers as described in Experimental Procedures

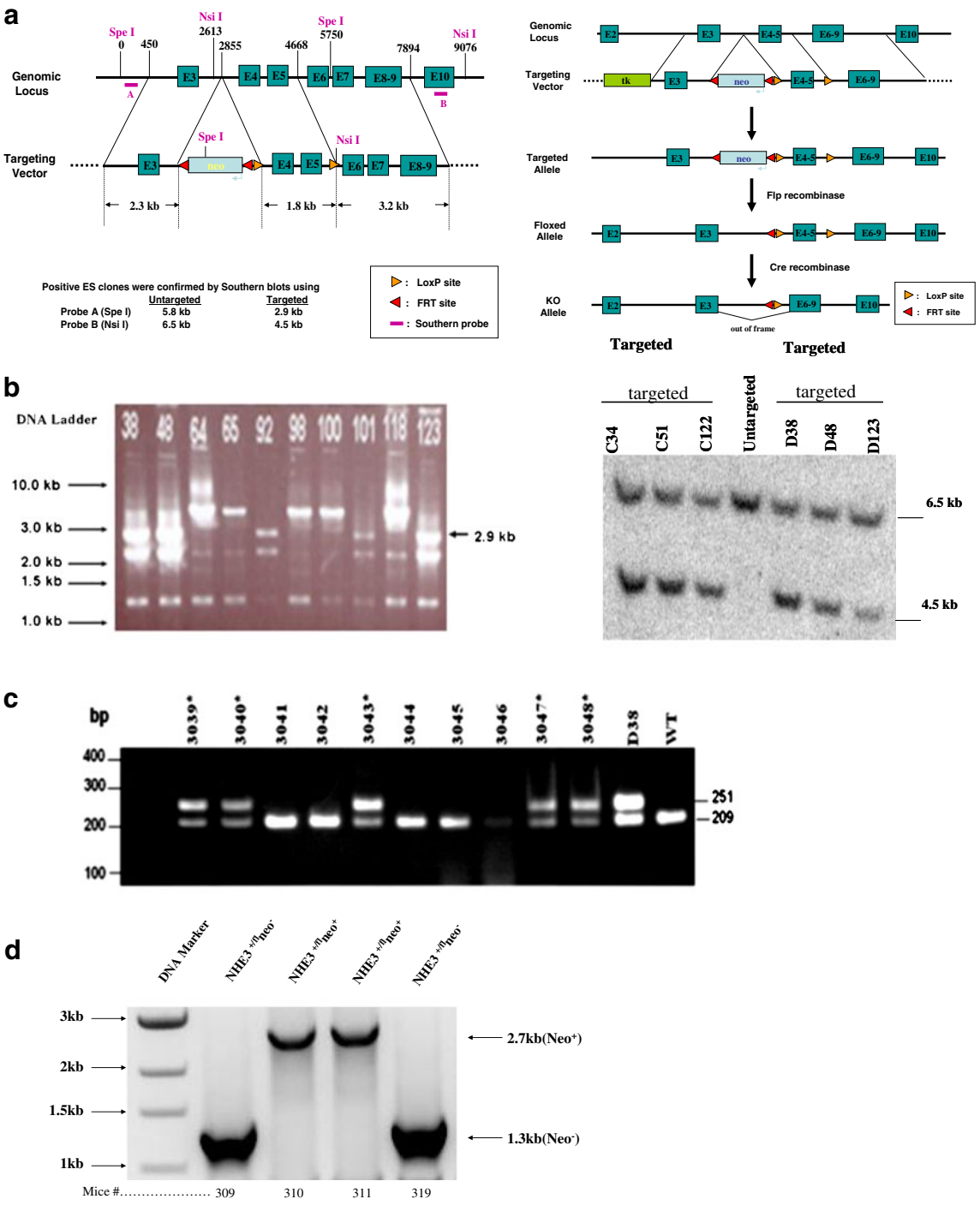

Generation of proximal tubule specific NHE3 KO mice (NHE3-PT KO) To generate proximal convoluted tubule-specific NHE3 KO mice, floxed NHE3 animals lacking the Neo Cassette were crossed with Sglt2 promoter-driven Cre recombinase transgenic mice [29]. A representative northern blot analysis demonstrates that NHE3 expression in the cortex is significantly reduced in $NHE3^{-/fl}/Cre^{+}$ (NHE3-PT KO) mice relative to $NHE3^{-/fl}$ mice (referred to as control; Fig. 2a, $p<0.05$, $n=3$). Immunofluorescence labeling revealed significant reduction in NHE3 expression in the kidney proximal tubule of NHE3-PT KO mice relative to control mice (Fig. 2b). Kidney histology of control and NHE3-PT KO mice did not show any remarkable differences.

Systemic acid base balance and systolic blood pressure in proximal tubule specific NHE3 KO mice To assess the role of proximal convoluted tubule NHE3 on systemic acid base

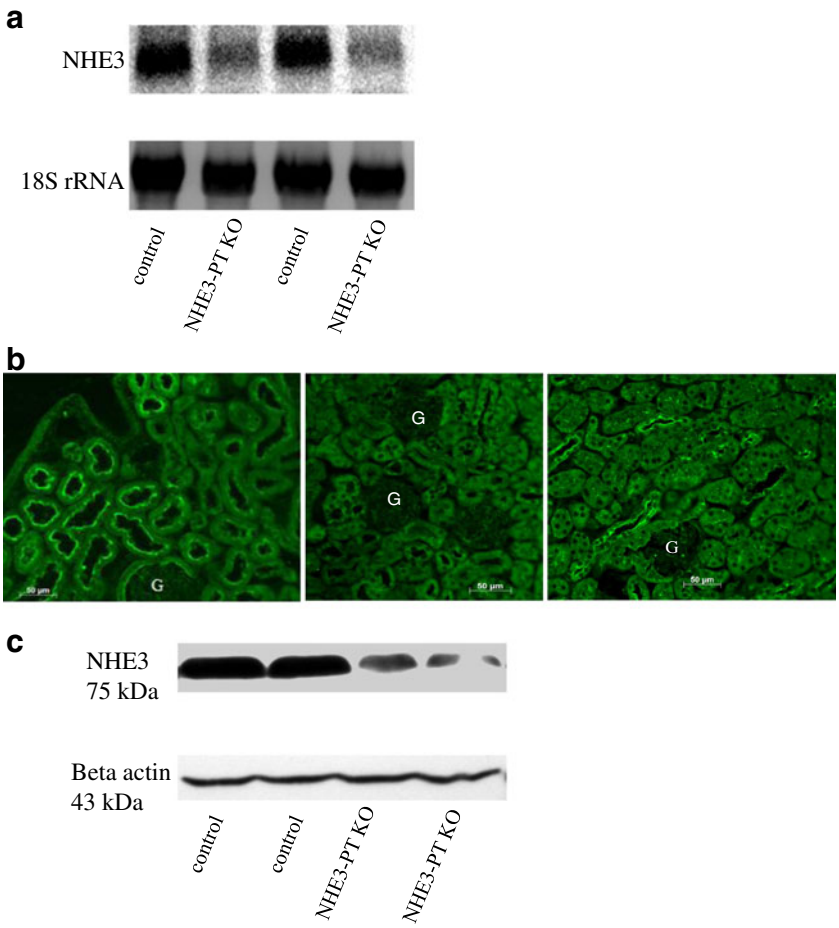

Fig. 2 Generation of proximal tubule specific NHE3 KO mice. **a** Northern hybridization. Representative northern blots demonstrate significant reduction in the expression of NHE3 mRNA in kidney cortices of two KO mice. **b** Immunofluorescence labeling. Immunofluorescence labeling revealed significant reduction in NHE3 expression in the kidney proximal tubule of NHE3-PT KO mice (*right panel*) relative to control mice (*left panel*). The complete absence of NHE3 in kidneys of conventional NHE3 KO mice (gifts from Dr. Shull) is shown for comparison (*middle panel*). **c** Western blot. Representative western blot shows significant reduction in the expression of NHE3 protein in kidney cortices of two KO mice (75 kDa). Equal loading was confirmed by determining the beta-actin levels (43 kDa, *lower panel*)

status, serum bicarbonate and pH were determined in NHE3-PT KO mice and control littermates. As shown in Fig. 3a, NHE3-PT KO mice have mild metabolic acidosis as determined by reduced serum bicarbonate (21.2 mEq/l in KO vs. 23.7 in WT, $p<0.05$, $n=5$ in each group) and arterial blood pH (7.23±0.02 in KO vs. 7.33±0.03 in WT, $p<0.05$, $n=5$). In comparison, the acid–base parameters measured in global NHE3 KO indicate that these animals have a more severe metabolic acidosis [24, 26] than the NHE3-PT KO mice. These results suggest that NHE3 located in the intestine and other nephron segments also plays a role in maintaining systemic acid–base balance. Blood pressure recording with the use of computerized tail cuff technique did not demonstrate any significant difference in the mean systolic blood pressure of control and NHE3-PT KO mice (Fig. 3b). Blood urea nitrogen levels were comparable in both genotypes (data not shown).

Reduced fluid and bicarbonate reabsorption in microperfused proximal tubules in NHE3-PT KO mice We examined NHE3 activity by measuring the rate of J_v and J_{HCO3} absorption in kidney proximal tubules of control ($NHE3^{-/fl}$) and NHE3-PT KO mice. Fluid absorption in proximal tubules was measured according to established protocols [36] and the bicarbonate absorption was examined by analyzing the change in total CO_2 concentrations between the original perfusate and the collected fluid [26]. Proximal tubules were isolated from WT and KO mice and perfused by using glucose-free Ringer solution to limit Na/glucose co-transporter activity and thereby allow the examination of Na/H-exchange activity in isolation. The tubular perfusion rate was 12±1 nl/min, which is similar to the normal single nephron GFR measured in mouse kidney [22]. The experimental results are summarized in Table 1 and shown in Fig. 4a and b. The perfusion rate, tubular length, J_v, and J_{HCO3} absorption in proximal tubules of control and NHE3-PT KO mice are included in Table 2. Results indicate that J_v was 0.92±0.06 and 0.67±0.07 nl/min/mm and J_{HCO3} was 83.09±9.73 and 53.52±4.62 pmol/min/mm in WT and in NHE3-PT KO proximal tubules, respectively. The J_{HCO3} was reduced 36 % and J_v was reduced 27 % in NHE3-PT KO compared to the control proximal tubules. The amount of reduction in J_{HCO3} is similar to our previous report in which the proximal tubule was isolated from total NHE3 KO mice, but the amount of reduction in J_v was less than our previous data [30]. These results indicate that both Na^+ and HCO_3^- absorption are reduced significantly in the NHE3-PT KO mice compared to control animals.

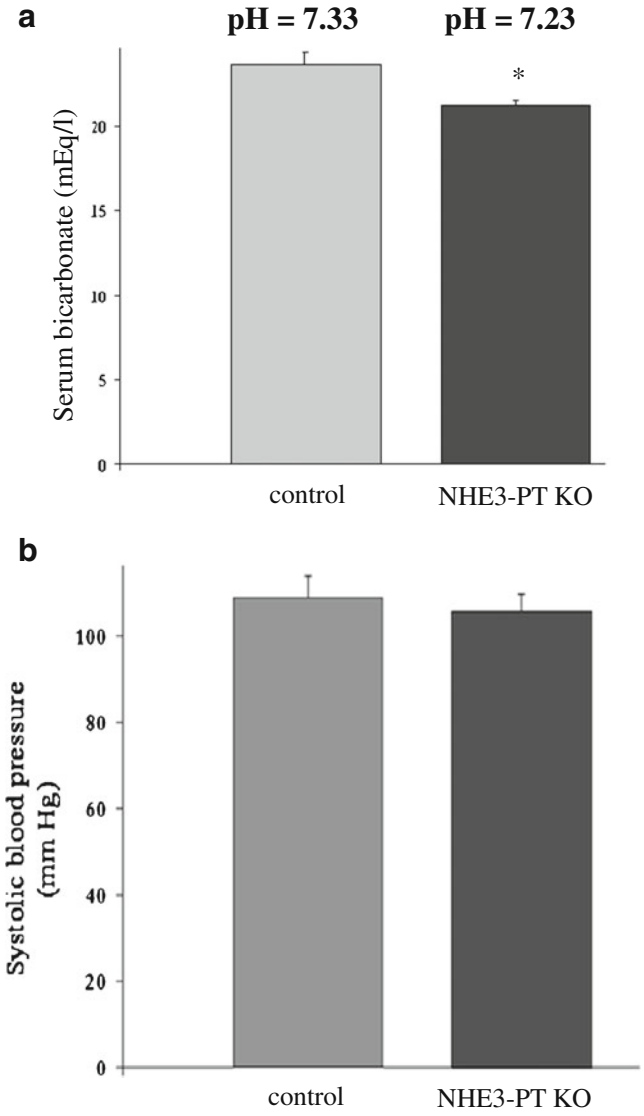

Fig. 3 Kidney function studies (systemic acid base balance and blood pressure). **a** Acid base balance studies. NHE3-PT KO mice have mild metabolic acidosis as determined by reduced serum bicarbonate and arterial blood pH compared to control animals. **b** Systolic blood pressure measurement. NHE3 PT KO mice do not display any notable reduction in systolic blood pressure compared to control mice ($p>0.05$ vs. control)

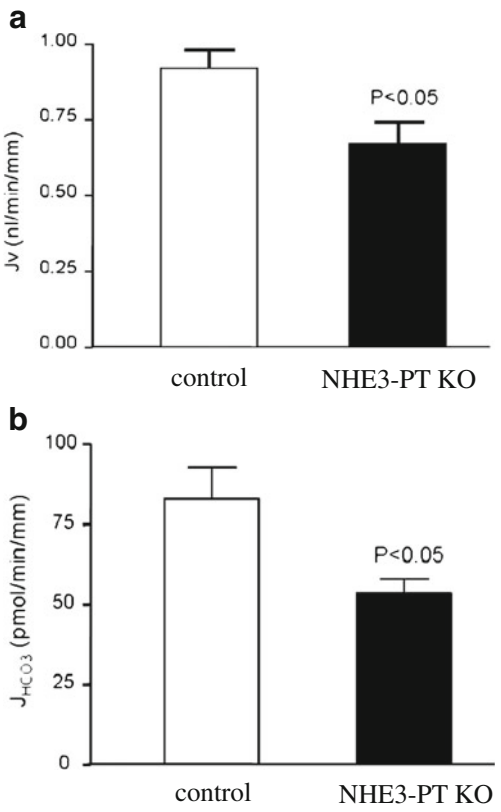

Fig. 4 Net fluid (J_v) and HCO_3^- (J_{HCO3}) absorption in microperfused proximal tubules of NHE3-PT KO and control mice. **a** Fluid absorption (J_v). In vitro microperfusion studies were performed as described in Experimental Procedures. The results demonstrated a ~27 % reduction in volume absorption in proximal tubules of NHE3-PT KO mice compared to their control littermates ($p<0.05$). **b** Bicarbonate absorption (J_{HCO3}). HCO_3^- absorption (J_{HCO3}) in microperfused proximal tubules was decreased by ~36 % reduction in NHE3-PT KO mice compared to their control littermates mice ($p<0.05$)

Urinary excretion of NH_4^+ in WT and NHE3-PT KO under control and acid load conditions In the next series of experiments we examined the role of kidney proximal tubule NHE3 in NH_4^+ (ammonium) excretion. These studies were designed based on published literature indicating that the apical Na^+/H^+ exchanger in the kidney proximal tubule can function in Na^+/NH_4^+ exchange mode (reviewed in 32). It was suggested that NHE3 could mediate the secretion of NH_4^+ into the lumen during conditions associated with enhanced ammoniagenesis, such as metabolic acidosis [37]. To test the role of proximal tubule NHE3 in NH_4^+ excretion, WT type and NHE3-PT KO mice were placed in metabolic cages and after acclimation were subjected to an acid load in the form of 280 mM NH_4Cl added to their drinking water. Urine output, water intake, and food intake were comparable in both genotypes before and after acid loading. Figure 5a depicts 24 h NH_4^+ excretion rate in WT and NHE3-PT KO at baseline, 2 and 5 days after acid loading. The baseline NH_4^+ excretion rates were comparable in WT and NHE3-PT KO mice (0.09±0.015 mmol/day in WT and 0.08±0.011 mmol/day in NHE3-PT KO mice, $p>0.05$, $n=5$). NH_4 excretion rate increased to 0.47± 0.10 mmol/day in WT and 0.46±0.1 mmol/day in NHE3-PT KO mice at 2 days after acid loading ($p>0.05$, $n=5$). At 5 days after acid loading, NH_4^+ excretion rates remained elevated at 0.50±0.06 mmol/day in WT and 0.36± 0.10 mmol/day in NHE3-PT KO mice.

Figure 5b depicts representative northern blot hybridization results comparing the renal expression of glutamine dehydrogenase, an essential enzyme in the synthesis of NH_4^+ in proximal tubule, after 5 days of acid loading. These results

Table 2 Summary of experiments examining bicarbonate and fluid absorption in proximal tubules of NHE3-PT KO and control mice

	N	Vo (nl/min)	L (mm)	$[HCO_3]_o$ (mM)	$[HCO_3]_L$ (mM)	J_v (nl/min/mm)	J_{HCO3} (pmol/min/mm)
$NHE3^{+/+}$	8	13.38±1.2	0.93±0.06	23.2±0.0	18.5±0.71	0.92±0.06	83.09±9.73
NHE3-PTKO	7	12.46±0.6	1.01±0.05	23.2±0.0	19.9±0.44	0.67±0.07*	53.52±4.61*

Values are means±SE

N number of perfused tubules, *Vo* perfusion rate, *L* tubular length, *[HCO3]$_o$* bicarbonate concentration in the original perfusate, *[HCO3]$_L$* bicarbonate concentration in collected fluid, J_v fluid reabsorption J_{HCO3} bicarbonate reabsorption

**$p<0.05$, significant difference from $PNHE3^{+/+}$ mice proximal tubules

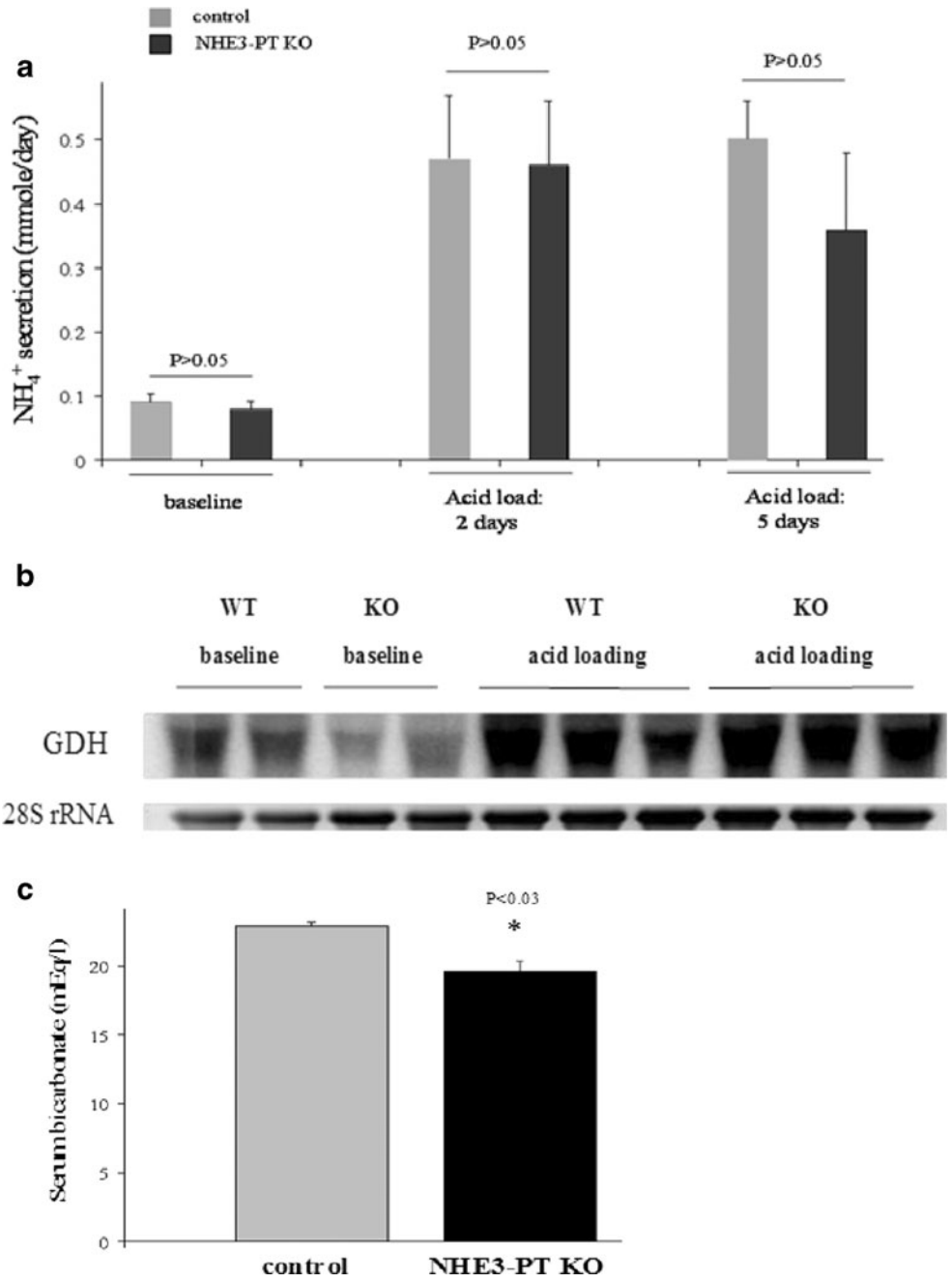

Fig. 5 Acid load challenge test in NHE3-PT KO and control mice. **a** Ammonium (NH_4^+) excretion. Twenty four-hour urine ammonium excretion rates were measured in NHE-PT KO and WT mice at baseline and in response to acid load. There was no significant difference in $NH4^+$ excretion rates in NHE3-PT KO and WT mice, either at baseline or in response to acid load at 2 or 5 days. **b** Expression of kidney glutamine dehydrogenase. Northern hybridizations indicated that the expression of GDH increases comparably in kidneys of NHE3-PT KO mice and their WT littermates after 5 days of acid loading. **c** Acid–base balance. Acid–base balance was determined in NHE-PT KO and WT mice in response to acid load after 5 days. There was no disproportionate acidosis in NHE3-PT KO mice beyond what was observed at baseline (Fig. 3)

indicate that the increase in expression of glutamine dehydrogenase is comparable in NHE3-PT KO and WT mice.

Figure 5c depicts the acid base status in NHE3-PT KO and WT animals in response to acid loading. As indicated, serum bicarbonate concentrations were 21.90±0.30 and 19.8±0.40 mEq/l in the WT and NHE3-PT KO mice, respectively ($p<0.03$), indicating that NHE3-PT KO mice did not develop disproportionate acidosis, which would have been the case if the ammoniagenesis pathway in these animals was dysfunctional.

In the next series of experiments, we examined the expression of NHE3 in the kidney medulla and small and large intestines of wild-type and proximal tubule-specific NHE3 KO mice. For comparison, NHE3 expression in global NHE3 KO mice was determined. Figure 6a shows the expression of NHE3 in the cortex and medulla of the wild type, proximal tubule specific KO (NHE3-PT KO) and global NHE3 KO mice. The results show significant upregulation of NHE3 in the medulla of NHE3-PT KO mice vs. wild-type animals (Fig. 6a). This adaptation predominantly reflects NHE3 upregulation in the thick ascending limb (and possibly the descending limb) in NHE3-PT KO mice. Contrary to the medulla, NHE3 expression shows significant reduction in NHE3-PT KO mice. The ablation of NHE3 in global NHE3 KO mice is shown for comparison. Figure 6b is a representative northern blot depicting NHE3 mRNA expression levels in jejunum (small intestine) and distal colon (large intestine) in wild type, proximal tubule-specific NHE3 KO and NHE3 global KO mice. The results show comparable NHE3 expression levels in intestines of wild-type and proximal tubule-specific NHE3 KO mice whereas no NHE3 was detected in intestines of global NHE3 KO mice.

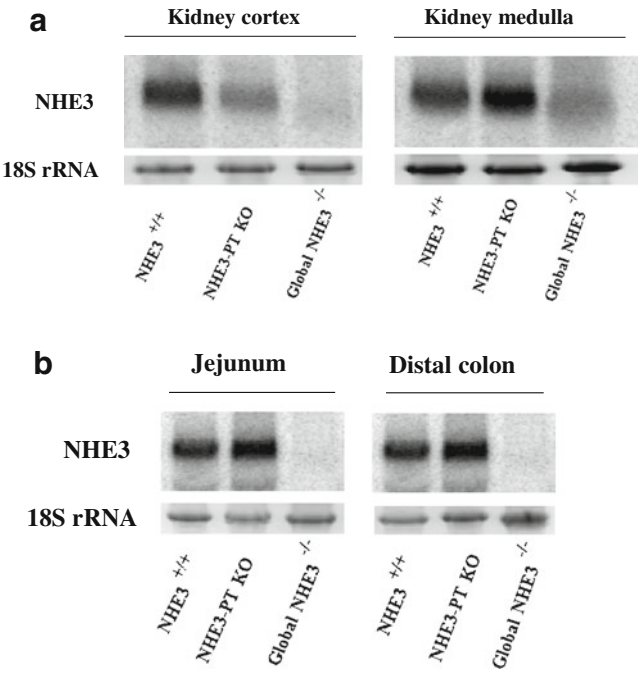

Fig. 6 Expression of NHE3 in the kidney and intestines of wild-type and proximal tubule specific NHE3 KO mice. **a** NHE3 expression in the kidney medulla. Representative northern blots demonstrate significant upregulation in the expression of NHE3 mRNA levels in kidney medulla of proximal tubule specific KO mice. Expression of NHE3 in the cortex is shown for comparison and shows significant reduction in proximal tubule specific KO mice. NHE3 expression in global NHE3 KO mice was completely absent. **b** NHE3 expression in the intestines. Representative northern blots demonstrating comparable NHE3 expression levels in jejunum and distal colon of wild-type and proximal tubule specific NHE3 KO mice. The absence of NHE3 expression in global NHE3 KO mice is shown for comparison. Similar patterns of expression were observed in the duodenum, ileum, and proximal colon

Discussion

NHE3 is expressed in numerous tissues, including intestine, stomach, brain, and kidney. It is regulated at both transcriptional and post-transcriptional levels and plays an important role in maintaining the systemic acid/base homeostasis. The ablation of NHE3 gene through conventional approach poses significant challenges with regard to assessment of its specific role in the kidney, mostly due to the fact that the mutant mice have significant vascular volume depletion resulting from the impairment of electrolyte absorption in the intestine [24]. This causes a number of changes, including a reduction in the kidney function or GFR and the activation of several pathways, including the rennin–angiotensin aldosterone system (RAS) [24]. The volume-associated reduction in GFR is also likely to increase the fractional reabsorption of various ions or molecules in the proximal tubule. Furthermore, the activation of RAS may alter the expression and/or activity of several ion and acid–base transporters such as H^+–ATPase and Na^+, K^+–ATPase in the kidney proximal tubules, NKCC2 in the thick ascending limb [38, 39]; NCC in the distal convoluted tubules; and AE1, AQP2, and epithelial sodium channel (ENaC) in the collecting duct [40–44]. Although transgenic $NHE3^{-/-}$($tgNHE3^{-/-}$) mice with the intestinal rescue-generated by overexpressing the rat NHE3 in NHE3 KO mice intestine showed increased absorption of Na^+ in the small intestine [45, 46], they still had global deletion of NHE3 in their kidney, complicating any conclusion with regard to the role of proximal convoluted tubule NHE3 in sodium and bicarbonate absorption (Table 2).

Mice with the proximal tubule specific NHE3 deletion (NHE3-PT KO) showed 36 and 27 % reduction in J_{HCO3} and J_v, respectively, in proximal tubules that were microperfused in vitro (Fig. 4, "Results" section). Previously, we reported that the Na^+ and HCO_3^- absorption was reduced by 63 and 54 %, respectively, in proximal tubules of global NHE3 KO mice perfused in vivo [26] and 46 and 34 %, respectively, when perfused in vitro [30]. The

baseline and NHE3-mediated fluid and HCO_3^- absorption in proximal tubules in vitro were lower than that in tubules perfused in vivo, indicating the proximal tubule likely functions better in vivo.

With regard to the in vitro microperfusion experiments in the two animal models (global NHE3 KO vs. proximal tubule specific NHE3 KO mice), we would like to indicate that NHE3 activity in the global NHE3 KO mice was examined in the presence of glucose in the tubular perfusate, whereas in NHE3-PT KO mice, glucose was eliminated in order to keep the Na-glucose cotransporter (Sglt1) idle. Therefore, while the reduction of J_{HCO3} was similar, 36 % (in the absence of glucose, Table 1) vs. 34 % (in the presence of glucose) [30] between global NHE3 KO and NHE3-PT KO, less profound reduction of J_v in the NHE3-PT KO compared to the WT in the absence of glucose (27 %, Table 1) compared to that in the presence of 10 mM of glucose (47 %) [47] suggests that either the Na-glucose cotransporter is upregulated in global NHE3 KO mice, or NHE3 is required for the Na/glucose cotransporter activation in proximal tubules. It has been reported that the expression of NaPi2 and AQP1 were increased in kidneys of global NHE3 KO mice [48], but whether these changes were secondary to the absence of NHE3 in the proximal tubule or were due to the impact of volume depletion or the activation of signaling pathways remain speculative. Examination of expression of the Na/glucose co-transporter, NaPi2 or AQP1 in kidneys of NHE3-PT KO mice will answer these questions.

The role of NHE3 in NH_4^+ (ammonium) secretion has been the subject of many studies. In carefully designed studies, Kinsella and Aronson demonstrated that the Na^+/H^+ exchanger in renal microvillus membrane vesicles has affinity for NH_4^+ and can mediate the exchange of Na^+ for H^+ or Na^+ for NH_4^+ [49]. It was concluded that the physiological significance of exchange modes other than Na^+/H^+ exchange was not certain at present, but Na^+/NH_4^+ exchange could play a role in the proximal tubular acidification process [49, 50]. Several studies in rodents have demonstrated that metabolic acidosis enhances the expression and activity of NHE3 in the proximal tubule [51–53]. Based on the above studies, it has been suggested that enhanced NHE3 expression can directly increase NH_4^+ secretion [37, 47, 50, 54].

In studies by Good and Burg, majority of NH_4 secretion was observed in S1 and S2 segment of the proximal tubules [17]. In studies by Nagami, it was suggested that S3 (straight) segment of the proximal tubule can also play a role in NH_4 secretion if AII is present [37, 55]. In proximal convoluted tubules microperfused in vitro, ammonia secretion into the lumen was found to be significantly inhibited by 0.1 mM amiloride in the presence of 10 mM Na in the perfusate when luminal pH was 7.4 [56]. However, the inhibitory effect of 0.1 mM amiloride on ammonia secretion was significantly diminished when the luminal pH was reduced to 6.2 in order to mimic in vivo conditions (above). Further, in separate studies, the effect of varying concentrations of potassium in bath or lumen on NH_4^+ secretion was found to be independent of the activity of Na^+/H^+ exchanger [57]. A recent report indicated that in neonate rats, metabolic acidosis increases NH_4^+ secretion, and upregulates the Na^+/H^+ exchanger NHE8 [58].

To determine if NHE3 is responsible for NH_4^+ secretion in the proximal tubule, we compared NH_4^+ excretion in NHE3-PT KO and WT mice under basal conditions and after 2 and 5 days of acid loading. Our data show no significant difference in NH_4^+ excretion between WT and NHE3-PT KO under either normal or acid loaded conditions. Acid loading with NH_4Cl increased the NH_4^+ secretion in both WT and NHE3-PT KO groups; however, the magnitude of increase was similar in both genotypes. Acid loading reduced serum HCO_3^- concentration by a similar magnitude (6.6 vs. 7.6 %, $p>0.05$) from baseline values in both WT and NHE3 PT KO mice. The absolute value of serum HCO_3^- concentration was lower in NHE3-PT KO than the WT mice (19.8 vs. 21.9 mEq/L, $p<0.03$), consistent with the acidosis phenotype in the KO mice.

The current studies directly assess the role of proximal convoluted tubule NHE3 in NH_4^+ secretion. Given the absence of any impairment in NH_4^+ excretion in NHE3-PT KO mice at baseline or during acidosis, we suggest that proximal convoluted tubule NHE3 (S1 and S2) alone does not have a significant impact on final NH_4^+ excretion in the urine. Whether other apical NHE isoforms (such as NHE8) are activated and play a role in NH_4^+ secretion in NHE3-PT KO mice remains to be determined. Lastly, whether the straight (S3) segment NHE3 can compensate for the lack of exchanger in the proximal convoluted tubule (S1 and S2) and play any role in NH_4^+ secretion in NHE3-PT KO mice remains speculative. Given the comparable expression level of enzymes involved in NH_4^+ generation in the proximal tubule in NHE3-PT KO and wild-type animals (Fig. 5), we suggest that the secretion of $NH3/NH_4^+$ into the lumen is independent of proximal convoluted tubule NHE3.

Published studies have shown that global NHE3 KO mice have severe phenotypes caused by the disruption of Na^+ and acid–base transport that are more profound than those observed in NHE3-PT KO animals. The significant reduction in blood pressure with elevated plasma aldosterone levels indicated that the impaired Na^+ absorption in the kidney proximal tubule cannot be fully compensated in global NHE3 KO mice, pointing to the importance of NHE3 in the intestine and other nephron segments [24]. In contrast, there was no significant reduction in blood pressure in NHE3-PT KO mice (Fig. 3), suggesting that the impaired NHE3-mediated Na^+ absorption in the proximal

tubule cannot be linked to reduced systemic blood pressure, a phenotype exhibited in global NHE3 KO mice as well as transgenic $NHE3^{-/-}$($tgNHE3^{-/-}$) mice with intestinal rescue [24, 45, 46]. When fed a regular NaCl diet, the transgenic $NHE3^{-/-}$($tgNHE3^{-/-}$) mice showed a lower ambulatory blood pressure compared to the wild-type controls ($tgNHE3^{+/+}$) [46]. This may be suggestive of a lack of NHE3 protein and impaired salt absorption in several nephron segments such as the proximal tubule (S3 segment) or the thick ascending limb in transgenic $NHE3^{-/-}$($tgNHE3^{-/-}$) mice [46].

The global NHE3 KO also showed more severe acidotic phenotype than that of NHE3-PT KO mice. The measured fresh arterial blood HCO_3^- was 20 % lower [26] and the serum HCO_3^- was 13 % lower [24] in global NHE3 KO than WT mice. In contrast, there is only a 10 % reduction of serum HCO_3^- in NHE3-PT KO compared to the WT mice. This latter observation is consistent with the specific loss of NHE3 function in the proximal tubule in NHE3-PT KO animal model. When compared to wild-type animals, NHE3 expression in the medulla (predominantly reflecting the thick ascending limb and possibly the descending limb) was found to be upregulated in the proximal tubule specific NHE3 KO mice (Fig. 6a), suggesting that enhanced salt absorption in the distal nephron might offset the reduction in salt absorption in the proximal tubule, thus minimizing the magnitude of salt wasting in the conditional KO mice. There was no impact of NHE3 deletion in the proximal tubule on NHE3 expression in intestines of proximal tubule specific NHE3 KO mice, as verified by normal NHE3 expression levels in the small and large intestines of proximal tubule specific KO mice (Fig. 6b).

In global NHE3 KO mice with NHE3 rescue in the small intestine, NHE3 is present in the small intestine at reduced levels but is completely absent in the large intestine [45, 46]. The global NHE3 KO mice show a significant upregulation of ENaC and colonic H-K-ATPase in their colon to compensate for the loss of NHE3 [24]. The expression levels of colonic H-K ATPase and ENaC in colons of the transgenic rescue model was not examined but we expect those to be elevated, due to the fact that in the transgenic rescue model the IFABP promoter which was used for the transgene expression is not expressed in the colon [45, 46]. We do not expect any altered expression in colonic H-K ATPase or ENaC in colons of proximal tubule NHE3 KO mice.

In conclusion, NHE3 plays an important role in bicarbonate reabsorption in the proximal convoluted tubule but does not play a significant role in NH_4 secretion, at least during the first 5 days of acid loading. The mild metabolic acidosis despite a significant reduction in net bicarbonate reabsorption in the proximal tubule of NHE3 KO mice is indicative of the presence of additional compensatory mechanisms in other nephron segments.

Acknowledgments These studies were supported by funds from the Center on Genetics of Transport and Epithelial Biology at the University of Cincinnati, a Merit Review award from the Department of Veterans Affairs, an NIH grant (R56DK 62809), and by grants from US Renal Care and DCI (to M.S).

References

1. Biemesderfer D, Pizzonia J, Abu-Alfa A, Exner M, Reilly R, Igarashi P, Aronson PS (1993) NHE3: a Na^+/H^+ exchanger isoform of renal brush border. Am J Physiol 265(5 Pt 2):F736–F742
2. Brant SR, Yun CHC, Donowitz M, Tse CM (1995) Cloning, tissue distribution, and functional analysis of the human Na^+/H^+ exchanger isoform, NHE3. Am J Physiol 269(38):C198–C206
3. Hoogerwerf WA, Tsao SC, Devuyst O, Levine SA, Yun CH, Yip JW, Cohen ME, Wilson PD, Lazenby AJ, Tse CM et al (1996) NHE2 and NHE3 are human and rabbit intestinal brush-border proteins. Am J Physiol 270(1 Pt 1):G29–G41
4. Maher MM, Gontarek JD, Bess RS, Donowitz M, Yeo CJ (1997) The Na^+/H^+ exchange isoform NHE3 regulates basal canine ileal Na^+ absorption in vivo. Gastroenterology 112(1):174–183
5. Cho JH, Musch MW, Bookstein CM, McSwine RL, Rabenau K, Chang EB (1998) Aldosterone stimulates intestinal Na^+ absorption in rats by increasing NHE3 expression of the proximal colon. Am J Physiol 274(3 Pt 1):C586–C594
6. Blanchard A, Eladari D, Leviel F, Tsimaratos M, Paillard M, Podevin RA (1998) $NH4^+$ as a substrate for apical and basolateral $Na(^+)$–H^+ exchangers of thick ascending limbs of rat kidney: evidence from isolated membranes. J Physiol 506(Pt 3):689–698
7. Kim GH, Ecelbarger C, Knepper MA, Packer RK (1999) Regulation of thick ascending limb ion transporter abundance in response to altered acid/base intake. J Am Soc Nephrol 10(5):935–942
8. Shah M, Gupta N, Dwarakanath V, Moe OW, Baum M (2000) Ontogeny of Na^+/H^+ antiporter activity in rat proximal convoluted tubules. Pediatr Res 48(2):206–210
9. Aronson PS (2002) Ion exchangers mediating NaCl transport in the renal proximal tubule. Cell Biochem Biophys 36(2–3):147–153
10. Watts BA 3rd, Good DW (1999) Hyposmolality stimulates apical membrane $Na(^+)/H(^+)$ exchange and HCO(3)(−) absorption in renal thick ascending limb. J Clin Invest 104(11):1593–1602
11. Capasso G, Unwin R, Rizzo M, Pica A, Giebisch G (2002) Bicarbonate transport along the loop of Henle: molecular mechanisms and regulation. J Nephrol 15(Suppl 5):S88–S96
12. Wang X, Armando I, Upadhyay K, Pascua A, Jose PA (2009) The regulation of proximal tubular salt transport in hypertension: an update. Curr Opin Nephrol Hypertens 18(5):412–420
13. Horita S, Seki G, Yamada H, Suzuki M, Koike K, Fujita T (2011) Insulin resistance, obesity, hypertension, and renal sodium transport. Int J Hypertens 2011:391762
14. Good DW, George T, Watts BA 3rd (2011) High sodium intake increases HCO(3)- absorption in medullary thick ascending limb through adaptations in basolateral and apical Na^+/H^+ exchangers. Am J Physiol Renal Physiol 301(2):F334–F343
15. Alexander RT, Grinstein S (2006) Na^+/H^+ exchangers and the regulation of volume. Acta Physiol (Oxf) Acta Physiol (Oxf) 187(1–2):159–167
16. Bobulescu IA, Moe OW (2006) Na^+/H^+ exchangers in renal regulation of acid–base balance. Semin Nephrol 26(5):334–344

17. Good DW, Burg MB (1984) Ammonia production by individual segments of the rat nephron. J Clin Invest 73(3):602–610
18. Kurtz I, Star R, Balaban RS, Garvin JL, Knepper MA (1986) Spontaneous luminal disequilibrium pH in S3 proximal tubules. Role in ammonia and bicarbonate transport. J Clin Invest 78(4):989–996
19. Vance BA, Biagi BA (1989) Microelectrode characterization of the basolateral membrane of rabbit S3 proximal tubule. J Membr Biol 108(1):53–60
20. Maunsbach AB, Vorum H, Kwon TH, Nielsen S, Simonsen B, Choi I, Schmitt BM, Boron WF, Aalkjaer C (2000) Immunoelectron microscopic localization of the electrogenic Na/HCO3 cotransporter in rat and ambystoma kidney. J Am Soc Nephrol 11:2179–2189
21. Amlal H, Chen Q, Greeley T, Pavelic L, Soleimani M (2001) Coordinated down-regulation of NBC-1 and NHE-3 in sodium and bicarbonate loading. Kidney Int 60:1824–1836
22. Lorenz JN, Schultheis PJ, Traynor T, Shull GE, Schnermann J (1999) Micropuncture analysis of single-nephron function in NHE3-deficient mice. Am J Physiol Ren Physiol 277:F447–F453
23. Collins JF, Xu H, Kiela PR, Zeng J, Ghishan FK (1997) Functional and molecular characterizationf of NHE3 expression during ontogeny in rat jejunal epithelium. Am J Physiol 273(6 Pt1): C1937–C1946
24. Schultheis PJ, Clarke LL, Meneton P, Miller ML, Soleimani M, Gawenis LR, Riddle TM, Duffy JJ, Doetschman T, Wang T et al (1998) Renal and intestinal absorptive defects in mice lacking the NHE3 Na^+/H^+ exchanger. Nat Genet 19:282–285
25. Amlal H, Ledoussal C, Sheriff S, Shull GE, Soleimani M (2003) Downregulation of renal AQP2 water channel and NKCC2 in mice lacking the apical Na^+–H^+ exchanger NHE3. J Physiol 533(2):511–522
26. Wang T, Yang CL, Abbiati T, Schultheis PJ, Shull GE, Giebisch G, Aronson PS (1999) Mechanism of proximal tubule bicarbonate absorption in NHE3 null mice. Am J Physiol Ren Physiol 277:298–302
27. Ledoussal C, Lorenz JN, Nieman ML, Soleimani M, Schultheis PJ, Shull GE (2001) Renal salt wasting in mice lacking NHE3 Na^+/H^+ exchanger but not in mice lacking NHE2. Am J Physiol Ren Physiol 281(4):F718–F727
28. Feng Y, Manka D, Wagner K-U, Khan SA (2007) Estrogen receptor-alpha expression in the mammary epithelium is required for ductal and alveolar morphogenesis in mice. Proc Natl Acad Sci 104(37):14718–14723
29. Rubera I, Poujeol C, Bertin G, Counillon L, Poujeol P, Tauc M (2004) Specific cre/lox recombination in the mouse proximal tubule. J Am Soc Nephrol 15:2050–2056
30. Du Z, Yan Q, Duan Y, Weinbaum S, Weinstein AM, Wang T (2006) Axial flow modulates proximal tubule NHE3 and H-ATPase activities by changing microvillus bending moments. Am J Physiol Ren Physiol 290:F289–F296
31. Barone S, Fussell SL, Singh AK, Lucas F, Xu J, Kim C, Wu X, Yu Y, Amlal H, Seidler U et al (2009) Slc2a5(Glut5) is essential for the absorption of fructose in the intestine and generation of fructose-induced hypertension. J Biol Chem 284(8):5056–5066
32. Xu J, Barone S, Li H, Holiday S, Zahedi K, Soleimani M (2011) Slc26a11, a chloride transporter, localizes with the vacuolar $H^{(+)}$-ATPase of A-intercalated cells of the kidney. Kidney Int 80(9):926–937
33. Yang L, Leong PK, Chen JO, Patel N, Hamm-Alvarez SF, McDonough AA (2002) Acute hypertension provokes internalization of proximal tubule NHE3 without inhibition of transport activity. Am J Physiol Ren Physiol 282(4):F730–F740
34. Yang LE, Leong PKK, McDonough AA (2007) Reducing blood pressure in SHR with enalapril provokes redistribution of NHE3, NaPi2, and NCC and decreases NaPi2 and ACE abundance. Am J Physiol Ren Physiol 293(4):F1197–F1208
35. Li HC, Szigligeti P, Worrell RT, Matthews JB, Conforti L, Soleimani M (2005) Missense mutations in Na^+: HCO_3^- cotransporter NBC1 show abnormal trafficking in polarized kidney cells: a basis of proximal renal tubular acidosis. Am J Physiol Ren Physiol 289(1):F61–F71
36. Burg MB, Orloff J (1968) Control of fluid absorption in the renal proximal tubule. J Clin Invest 47(9):2016–2024
37. Nagami GT (2008) Role of angiotensin II in the enhancement of ammonia production and secretion by the proximal tubule in metabolic acidosis. Am J Physiol Ren Physiol 294(4):F874–F880
38. Garg LC (1991) Respective roles of H-ATPase and H-K-ATPase in ion transport in the kidney. J Am Soc Nephrol 2(5):949–960
39. Takahashi N, Chernavvsky DR, Gomez RA, Igarashi P, Gitelman HJ, Smithies O (2000) Uncompensated polyuria in a mouse model of Bartter's syndrome. Proc Natl Acad Sci USA 97:5434–5439
40. Simon DB, Nelson-Williams C, Bia MJ, Ellison D, Karet FE, Molina AM, Vaara I, Iwata F, Cushner HM, Koolen M et al (1996) Gitelman's variant of Bartter's syndrome, inherited hypokalaemic alkalosis, is caused by mutations in the thiazide-sensitive Na-Cl cotransporter. Nat Genet 12(1):24–30
41. Devonald MA, Smith AN, Poon JP, Ihrke G, Karet FE (2003) Non-polarized targeting of AE1 causes autosomal dominant distal renal tubular acidosis. Nat Genet 33:125–127
42. Cantone A, Yang X, Yan Q, Giebisch G, Hebert SC, Wang T (2008) Mouse model of type II Bartter's syndrome. I. Upregulation of thiazide-sensitive Na-Cl cotransport activity. Am J Physiol Ren Physiol 294:F1366–F1372
43. Bankir L, Bichet DG, Bouby N (2010) Vasopressin V2 receptors, ENaC, and sodium reabsorption: a risk factor for hypertension? Am J Physiol Renal Physiol 299(5):F917–F928
44. Soleimani M, Barone S, Xu J, Shull GE, Siddiqui F, Zahedi K, Amlal H (2012) Double knockout of pendrin and Na-Cl cotransporter(NCC) causes severe salt wasting, volume depletion, and renal failure. Proc Natl Acad Sci U S A 109(33):13368–13373
45. Woo AL, Noonan WT, Schultheis PJ, Neumann JC, Manning PA, Lorenz JN, Shull GE (2003) Renal function in NHE3-deficient mice with transgenic rescue of small intestinal absorptive defect. Am J Physiol Ren Physiol 284(6):F1190–F1198
46. Noonan WT, Woo AL, Nieman ML, Prasad V, Schultheis PJ, Shull GE, Lorenz JN (2005) Blood pressure maintenance in NHE3-deificient mice with transgenic expression of NHE3 in small intestine. Am J Physiol Regul Integr Comp Physiol 288(3):R685–R691
47. Karim Z, Szutkowska M, Vernimmen C, Bichara M (2006) Recent concepts concerning the renal handling of $NH3/NH4^+$. J Nephrol 19(Suppl 9):S27–S32
48. Brooks HL, Sorensen AM, Terris J, Schultheis PJ, Lorenz JN, Shull GE, Knepper MA (2001) Profiling of renal tubule Na^+ transporter abundances in NHE3 and NCC null mice using targeted proteomics. J Physiol 530(3):359–366
49. Kinsella JL, Aronson PS (1981) Interaction of $NH4^+$ and Li^+ with the renal microvillus membrane Na^+–H^+ exchanger. Am J Physiol 241(5):C220–C226
50. Paillard M (1997) Na^+/H^+ exchanger subtypes in the renal tubule: function and regulation in physiology and disease. Exp Nephrol 5(4):277–284
51. Ambühl PM, Amemiya M, Danczkay M, Lötscher M, Kaissling B, Moe OW, Preisig PA, Alpern RJ (1996) Chronic metabolic acidosis increases NHE3 protein abundance in rat kidney. Am J Physiol 271(4 Pt2):F917–F925
52. Wu MS, Biemesderfer D, Giebisch G, Aronson PS (1996) Role of NHE3 in mediating renal brush border Na^+−H^+ exchanger. Adaptation to metabolic acidosis. J Biol Chem 271(51):32749–32752

53. Laghmani K, Preisig PA, Moe OW, Yanagisawa M, Alpern RJ (2001) Endothelin-1/endothelin-B receptor-mediated increases in NHE3 activity in chronic metabolic acidosis. J Clin Invest 107(12):1563–1569
54. Weiner ID, Verlander JW (2011) Role of NH3 and $NH4^+$ transporters in renal acid–base transport. Am J Physiol Ren Physiol 300(1):F11–F23
55. Nagami GT (2004) Ammonia production and secretion by S3 proximal tubule segments from acidotic mice: role of ANG II. Am J Physiol Ren Physiol 287(4):F707–F712
56. Nagami GT (1988) Luminal secretion of ammonia in the mouse proximal tubule perfused in vitro. J Clin Invest 81(1): 159–164
57. Nagami GT (1990) Effect of bath and luminal potassium concentration on ammonia production and secretion by mouse proximal tubules perfused in vitro. J Clin Invest 86(1):32–39
58. Twombley K, Gattineni J, Bobulescu IA, Dwarakanath V, Baum M (2010) Effect of metabolic acidosis on neonatal proximal tubule acidification. Am J Physiol Regul Integr Comp Physiol 299(5): R1360–R1368